

Analytical solution of Rayleigh-Taylor instability in a Hall thruster having double-ionized ions

Dhananjay Verma*, Hitendra K. Malik

Plasma Science and Technology Laboratory, Department of Physics, Indian Institute of Technology Delhi, New Delhi, India.

*Corresponding author: dhananjayverma3510@gmail.com

Received 08 July 2023; Accepted 16 August 2023; Published Online 20 October 2023

ORIGINAL RESEARCH

Abstract:

A modified Rayleigh-Taylor (RT) instability equation is derived using a three-fluid Hall thruster plasma model by including multi-ionized ions to study the growth rate of the RT instability. For a simplified plasma density and electron drift velocity axial profile, the growth rate for an unstable wave and the condition leading to this instability are discussed. A possible analytical solution for the modified Rayleigh-Taylor equation is discussed along with the condition that leads to it. For double-ionized ions, the behavior of growth rate and perturbed potential for different densities of double-ionized ions are studied.

Keywords: Multi-ionized ions; Instability conditions; Density-driven instability; Solution of modified Rayleigh-Taylor equation

1. Introduction

Hall thrusters are the electric propulsion systems that fall among the most promising electric propulsion devices due to their high specific impulse, zero limitation on ion current density, higher efficiency, and longer operating time [1]. Electric thruster takes less power to operate, and this can be achieved by solar energy. These devices are relatively smaller than the conventional rocket engines and use less fuel. The Hall thrusters can attain very high speed in space (provided continuous operation for a long time), making them ideal for space applications and a valid candidate for interplanetary travel. These electric thrusters are known to provide the thrust of the order of mN to 1N, which is not much, but their continuous operation for a longer period is enough for the satellite adjustment in outer space.

An axial electric field from a grided anode toward a heated cathode and a radial magnetic field in an annular channel are the main elements of a Hall thruster or closed drift thruster (Fig. 1). The applied radial magnetic field and the axial electric field cause the electrons coming from the cathode to be trapped and drift in the azimuthal direction (thus, the name close drift thruster). These azimuthally drifting electrons collide with the neutral gas atoms injected from the anode, generating plasma. Heavy and unmagnetized ions acceler-

ate toward the cathode by the axial electric field while the electrons stay trapped by the magnetic field. These accelerated ions get neutralized by the heated cathode so that they are not pulled back and keep on producing the thrust [1, 2]. The oscillations and instabilities inside the Hall thruster plasma affect the electron transport, their energy transport, wall erosion rate, and plasma plume (directly the thrust); in other words, they affect the efficiency of the Hall thruster and reduce its lifespan [3]. The main reason for these instabilities and oscillations are different drift velocities of electrons and ions, density gradient, and nonuniformity of the magnetic field [2]. In the past years, several studies have been done regarding various Hall thruster plasma modeling, magnetic configuration, plasma plume, electron transport, and instabilities, both theoretically and experimentally [4, 5].

Inside the thruster channel, the plasma is formed at the ionization front of trapped electrons, generating a density gradient in the system. The radial magnetic field holds this density gradient. As the system is in the state of higher potential energy, any fluctuations in the density gradient will grow in such a way that the system goes into relatively lower potential energy. Thus, any fluctuation in the axial density gradient will grow into instability, called Rayleigh-Taylor instability. Litvak and Fisch have stud-

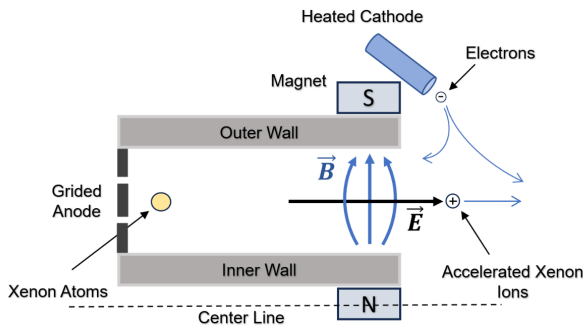


Figure 1. Schematic representation of Hall Thruster, showing the inner and outer walls of the acceleration channel and the electric and magnetic fields.

ied the gradient-driven Rayleigh-Taylor instability (of MHz range) in a Hall thruster by neglecting the temperature of electrons and ions and found a special case solution using a step-like profile of the plasma parameters [6]. The temperature of the electrons inside a Hall thruster operating at a discharge voltage of 300 V is high enough to multi-ionize the neutral Xenon gas atoms [7]. Also, an increased density of multi-ionized ions leading to a lower wall erosion rate has been observed by Kim et al. while studying the magnetic field tailoring effect [3]. As the neutral Xenon atoms are injected from the anode side, they collide with the electrons drifting azimuthally and get ionized. On further collisions with the electrons accelerating toward the anode, multi-ionization of Xenon atoms takes place. Because ions are heavy and unmagnetized, they help into breaking the magnetic confinement of the electrons which fall in their Debye sphere, reducing the density gradient. Since the Debye sphere of double-ionized ions has more charge in it, these ions will reduce the density gradient even more. The increased density of double-ionized ions inside the channel also represents increased ionization, resulting in a lower axial gradient in the density of electrons. These will reduce the Rayleigh-Taylor instability growth rate. Thus, in this article, a modified Rayleigh-Taylor instability is being studied while including the electron and ion temperatures in the presence of ions with double-ionization using a three-fluid plasma model. An analytical approach is used to get the growth rate of the unstable wave along with the axial profile of perturbing potential, which is also confirmed with the help of numerical solution of the modified Rayleigh-Taylor equation.

2. Mathematical model

To investigate the Rayleigh-Taylor instability present in a Hall thruster plasma, a two-dimensional thruster model is used by neglecting the azimuthal curvature and considering zero variations in thruster parameters along the radial direction of the thruster channel. The accelerating electric field \mathbf{E} is taken along the x -axis and the radial magnetic field $\mathbf{B} = B_0\hat{z}$ along the z -axis to trap the electrons, giving rise to an electron drift along the y -axis while the ions are accelerated along the x -axis. In the current investigation, a three-fluid plasma model comprising magnetized electrons, unmagnetized singly ionized ions, and cold double-ionized

ions is used to investigate the instability corresponding to azimuthally propagating wave. The effects of collisions are not studied in the current investigation, and electrons and ions are taken to have a uniform temperature while double-ionized ions are considered to be cold as their accelerating velocity are very high compared to their thermal velocity. The motions of ions and electrons are governed by fluid equations. The equations of motion and continuity equation for the ions (singly and double-ionized) fluid are given by

$$\frac{\partial \mathbf{v}_i}{\partial t} + (\mathbf{v}_i \cdot \nabla) \mathbf{v}_i = \frac{e\mathbf{E}}{M} - \frac{\nabla p_i}{Mn_i} \quad (1)$$

$$\frac{\partial n_i}{\partial t} + \nabla \cdot (n_i \mathbf{v}_i) = 0 \quad (2)$$

$$\frac{\partial \mathbf{v}_{zi}}{\partial t} + (\mathbf{v}_{zi} \cdot \nabla) \mathbf{v}_{zi} = \frac{2e\mathbf{E}}{M} \quad (3)$$

$$\frac{\partial n_{zi}}{\partial t} + \nabla \cdot (n_{zi} \mathbf{v}_{zi}) = 0 \quad (4)$$

Here, M is the mass of the ions (for both singly and double-ionized), and z represents the level of ionization of the multi-ionized ions.

To find the growth rate of the instability, a small perturbation is added in the density, fluid velocity, and electric field and see whether it grows or dies out with time. The unperturbed fluid velocity for the electrons and the ions are along the y - and x -axes, represented by u_0 and v_{i0} (v_{zi0} for double-ionized ions). After linearization, the Equations (1)-(4) become

$$\frac{\partial \mathbf{v}_{i1}}{\partial t} + v_{i0} \frac{\partial \mathbf{v}_{i1}}{\partial x} = \frac{-e\nabla \phi_1}{M} - \frac{\gamma_i k_B T_i \nabla (n_{i0} + n_{i1})}{Mn_{i0}} \quad (5)$$

$$\frac{\partial n_{i1}}{\partial t} + n_{i0} (\nabla \cdot \mathbf{v}_{i1}) + v_{i0} \frac{\partial n_{i1}}{\partial x} = 0 \quad (6)$$

$$\frac{\partial \mathbf{v}_{zi1}}{\partial t} + v_{zi0} \frac{\partial \mathbf{v}_{zi1}}{\partial x} = \frac{-2e\nabla \phi_1}{M} \quad (7)$$

$$\frac{\partial n_{zi1}}{\partial t} + n_{zi0} (\nabla \cdot \mathbf{v}_{zi1}) + v_{zi0} \frac{\partial n_{zi1}}{\partial x} = 0 \quad (8)$$

Here γ_i , called the heat capacity ratio, is the ratio of heat capacity at constant pressure to the heat capacity at constant volume for ion fluids as they are considered to be monoatomic particles in a two-dimensional space and k_B is the Boltzmann constant. The terms with subscript 0 represent the unperturbed quantity, and those with subscript 1 represent the perturbed quantity. The electric field can be represented in the form of electrostatic potential as $E = -\nabla \phi$. And a small perturbation in the potential is represented as $\phi = \phi_0 + \phi_1$, where ϕ_0 represents the unperturbed potential which is 0. Let these perturbing quantities have a sinusoidal form of

$$A_1 = A_0 e^{(i\omega t - ik_y y)} \quad (9)$$

Here ω and k_y are the frequency of the perturbing wave and its wave number. After solving Equations (5) and (7) for the ion's velocity with the help of Equation (9) and using those expressions in Equations (6) and (8), the ion's perturbed densities are obtained as

$$n_{i1} = \frac{en_{i0}}{M\omega^2 - \gamma_i T_i k_y^2} \left(k_y^2 \phi_1 - \frac{\partial^2 \phi_1}{\partial x^2} - \frac{\gamma_i k_B T_i}{en_{i0}} \frac{\partial^2 n_{i0}}{\partial x^2} \right) \quad (10)$$

$$n_{zi1} = \frac{zen_{zi0}}{M\omega^2} \left(k_y^2 \phi_1 - \frac{\partial^2 \phi_1}{\partial x^2} \right) \tag{11}$$

Now, the fluid equations for the magnetized electrons are given by

$$\frac{\partial \mathbf{u}_e}{\partial t} + (\mathbf{u}_e \cdot \nabla) \mathbf{u}_e = -\frac{e}{m} (\mathbf{E} + \mathbf{u}_e \times \mathbf{B}) - \frac{\nabla p_e}{mn_e} \tag{12}$$

$$\frac{\partial n_e}{\partial t} + \nabla \cdot (n_e \mathbf{u}_e) = 0 \tag{13}$$

Here \mathbf{u}_e and n_e are the electron fluid velocity and density, and m is the electron's mass. The unperturbed electron drift velocity u_0 depends on the magnetic field profile; thus, it has an axial profile as the magnetic field. After linearization, Equations (12) and (13) are transformed to

$$\frac{\partial \mathbf{u}_{e1}}{\partial t} + u_0 \frac{\partial \mathbf{u}_{e1}}{\partial y} + u_{e1x} \frac{\partial \mathbf{u}_0}{\partial x} = -\frac{e}{m} (-\nabla \phi_1 + \mathbf{u}_{e1} \times \mathbf{B}) - \frac{\gamma_e k_B T_e \nabla (n_{e0} + n_{e1})}{mn_{e0}} \tag{14}$$

$$\frac{\partial n_{e1}}{\partial t} + n_{e0} (\nabla \cdot \mathbf{u}_{e1}) + \frac{\partial n_{e0}}{\partial x} u_{e1x} + u_0 \frac{\partial n_{e1}}{\partial y} = 0 \tag{15}$$

Here, γ_e is the specific heat ratio for the electron fluid. We get the x - and y - components of the electrons' fluid velocity after using the condition $\Omega \gg \omega, k_y u_0, \partial u_0 / \partial x$ from Equation (14) with the help of Equation (9). Here $\Omega = eB_0/m$ is the electron cyclotron frequency and $u_0 = |E_0/B_0|$ is the electron drift velocity in the azimuthal direction.

$$u_{1x} = \frac{e}{m\Omega^2} \left[i(\omega - k_y u_0) \frac{\partial \phi_1}{\partial x} + ik_y \Omega \phi_1 - ik_y \Omega \frac{\gamma_e k_B T_e}{en_{e0}} n_{e1} - i(\omega - k_y u_0) \frac{\gamma_e k_B T_e}{en_{e0}} \frac{\partial n_{e0}}{\partial x} + ik_y \phi_1 \frac{\partial u_0}{\partial x} - ik_y \frac{\gamma_e k_B T_e}{en_{e0}} \frac{\partial u_0}{\partial x} n_{e1} \right] \tag{16}$$

$$u_{1y} = \frac{e}{m\Omega} \left(\frac{\partial \phi_1}{\partial x} - \frac{\gamma_e k_B T_e}{en_{e0}} \frac{\partial n_{e0}}{\partial x} + \frac{k_y (\omega - k_y u_0) \phi_1}{\Omega} - \frac{k_y (\omega - k_y u_0)}{\Omega} \frac{\gamma_e k_B T_e}{en_{e0}} n_{e1} \right) \tag{17}$$

Using Equations (16) and (17) in Equation (15), along with Equation (9), the electron's perturbed density is obtained as

$$n_{e1} = \frac{\left\{ \frac{en_{e0}}{m\Omega^2} \left[(\omega - k_y u_0) (k_y^2 \phi_1 - \frac{\partial^2 \phi_1}{\partial x^2}) - k_y \xi(x) \phi_1 \right] - \frac{\gamma_e k_B T_e}{m\Omega} \left[k_y \frac{\partial n_{e0}}{\partial x} - \frac{(\omega - k_y u_0)}{\Omega} \frac{\partial^2 n_{e0}}{\partial x^2} \right] \right\}}{(\omega - k_y u_0) \left[1 + \frac{\gamma_e k_B T_e k_y}{m\Omega^2 (\omega - k_y u_0)} (k_y (\omega - k_y u_0) - \xi(x)) \right]} \tag{18}$$

where $\xi(x) = \partial^2 u_0 / \partial x^2 + \Omega / n_{e0} (\partial n_{e0} / \partial x)$. Now, the perturbed ions, double-ionized ions, and electron densities from Equations (10), (11), and (18) are used in Poisson's equation $\nabla^2 \phi_1 = e / \epsilon_0 (n_{e1} - n_{i1} - 2n_{zi1})$. This

gives the following equation in the perturbed potential

$$\left(\frac{\partial^2 \phi_1}{\partial x^2} - k_y^2 \phi_1 \right) \left[1 + \frac{\omega_{pe}^2 (\omega - k_y u_0)}{(\omega - k_y u_0) Q} - \frac{\omega_{pi}^2}{\omega^2 - v_{thi}^2 k_y^2} - \frac{\omega_{pzi}^2}{\omega^2} \right] + \frac{\frac{\omega_{pe}^2}{\Omega^2} k_y \xi(x) \phi_1 + \frac{u_{the}^2}{\epsilon_0 \Omega} \left[k_y \frac{\partial n_{e0}}{\partial x} - \frac{(\omega - k_y u_0)}{\Omega} \frac{\partial^2 n_{e0}}{\partial x^2} \right]}{(\omega - k_y u_0) Q} - \frac{\omega_{pi}^2}{(\omega^2 - v_{thi}^2 k_y^2)} \frac{\gamma_i k_B T_i}{en_{i0}} \frac{\partial^2 n_{i0}}{\partial x^2} = 0, \text{ where}$$

$$Q = \left[1 + \frac{\gamma_e T_e k_y}{m\Omega^2 (\omega - k_y u_0)} (k_y (\omega - k_y u_0) - \xi(x)) \right]. \tag{19}$$

Here, $\omega_{pe}^2 = (n_{e0} e^2) / (\epsilon_0 m)$, $\omega_{pi}^2 = (n_{i0} e^2) / (\epsilon_0 M)$, and $\omega_{pzi}^2 = (4n_{zi0} e^2) / (\epsilon_0 m)$ are the plasma oscillation frequencies for electrons, singly ionized and multi-ionized ions. The thermal velocities of the electron and single-ionized ions are given by $u_{the}^2 = \gamma_e k_B T_e / m$ and $v_{thi}^2 = \gamma_i k_B T_i / M$.

3. Growth rate

Now, to get the dispersion relation of this azimuthal propagating wave, the unperturbed part of Equation (19) is solved. Thus, the following expression is needed to be solved for the plasma wave modes and their growth rate.

$$\frac{e}{\epsilon_0} \frac{u_{the}^2}{\Omega} \left[k_y \frac{\partial n_{e0}}{\partial x} - \frac{(\omega - k_y u_0)}{\Omega} \frac{\partial^2 n_{e0}}{\partial x^2} \right] (\omega - k_y u_0) \left[1 + \frac{\gamma_e k_B T_e k_y}{m\Omega^2 (\omega - k_y u_0)} (k_y (\omega - k_y u_0) - \xi(x)) \right] - \frac{\omega_{pi}^2}{(\omega^2 - v_{thi}^2 k_y^2)} \frac{\gamma_i k_B T_i}{en_{i0}} \frac{\partial^2 n_{i0}}{\partial x^2} = 0 \tag{20}$$

On simplifying Equation (20), the dispersion relation is given by

$$\left[\frac{\partial^2 n_{e0}}{\partial x^2} \right] \omega^3 - \left[k_y \Omega \frac{\partial n_{e0}}{\partial x} + k_y u_0 \frac{\partial^2 n_{e0}}{\partial x^2} \right] \omega^2 + \left[-\frac{\partial^2 n_{e0}}{\partial x^2} k_y^2 v_{thi}^2 + v_{thi}^2 \frac{\partial^2 n_{i0}}{\partial x^2} \left(k_y^2 + \frac{\Omega^2}{u_{the}^2} \right) \right] \omega + \left[k_y \Omega \frac{\partial n_{e0}}{\partial x} + k_y u_0 \frac{\partial^2 n_{e0}}{\partial x^2} \right] k_y^2 v_{thi}^2 - \left[k_y u_0 \left(k_y^2 + \frac{\Omega^2}{u_{the}^2} \right) + k_y (\xi(x)) \right] v_{thi}^2 \frac{\partial^2 n_{i0}}{\partial x^2} = 0 \tag{21}$$

Equation (21) is a third-degree polynomial that is solved for the frequency ω which gives rise to three distinctive solutions

$$a_3 \omega^3 + a_2 \omega^2 + a_1 \omega + a_0 = 0 \tag{22}$$

where a_3, a_2, a_1 and a_0 are the coefficients of $\omega^3, \omega^2, \omega^1$ and ω^0 respectively in the Equation (21). Equation (22) is solved by eliminating the term containing ω^2 and then transforming it into a quadratic equation. This is done by replacing ω with $y - (a_2/3a_3)$, where y is a variable. It gives

$$y^3 + 3py - 2q = 0$$

Now, replacing y with $u - (p/u$, where u is a new variable, we get

$$(u^3)^2 - 2q(u^3) - p^3 = 0$$

This equation has a solution $u^3 = q \pm \sqrt{q^2 + p^3}$ and it is further solved for all the three solutions, which are

$$\omega_1 = r^{\frac{1}{3}} - pr^{-\frac{1}{3}} - \frac{a_2}{3a_3},$$

$$\omega_2 = \frac{1}{2} \left(-r^{\frac{1}{3}} + pr^{-\frac{1}{3}} - \frac{2a_2}{3a_3} \right) + i \frac{\sqrt{3}}{2} \left(r^{\frac{1}{3}} + pr^{-\frac{1}{3}} \right),$$

$$\omega_3 = \frac{1}{2} \left(-r^{\frac{1}{3}} + pr^{-\frac{1}{3}} - \frac{2a_2}{3a_3} \right) - i \frac{\sqrt{3}}{2} \left(r^{\frac{1}{3}} + pr^{-\frac{1}{3}} \right).$$

where $p = \frac{3a_3a_1 - a_2^2}{9a_3^2}$, $q = \frac{9a_3a_2a_1 - 27a_3^2a_0 - 2a_2^3}{54a_3^3}$

and $r = q + \sqrt{q^2 + p^3}$.

As we are interested in the unstable mode of plasma waves and the solution of a third-degree polynomial will have one real and two complex solutions only if the following condition is met

$$q^2 + p^3 > 0 \tag{23}$$

otherwise, all the solutions will be real. So, there will not be any Rayleigh-Taylor instability present in the system unless the condition stated in Equation (23) is achieved.

Here, it is observed that the frequency ω_1 is real and ω_2 and ω_3 are complex. It is further observed that only $\omega_3 = (\omega_R - i\omega_I)$ can provide an unstable plasma wave. Finally, the growth rate of the Rayleigh-Taylor wave is given by

$$\gamma = \frac{\omega_R}{\omega_{pi}} = \frac{\frac{\sqrt{3}}{2} \left(r^{\frac{1}{3}} + pr^{\frac{1}{3}} \right)}{\omega_{pi}} \tag{24}$$

The dependency of the growth rate γ on various plasma parameters can be given by Equation (24). The growth rate comes out to be $\gamma = 0.0264$ for the plasma density of $10^{18}/m^3$, radial magnetic field strength B of 0.021 T and 60% double-ionized ions, while the other parameters are the same as of Figure 1 which are used in the Hall thruster studies. If the magnetic field strength B is increased to 0.026 T, then the growth rate γ increases to 0.0399. The increased gradient causes this increase in the growth rate, revealing that it is the gradient driven Rayleigh-Taylor instability. If the plasma density is decreased to $10^{17}/m^3$ the growth rate γ is increased to 0.0836; similar behaviour is seen on decreasing the density of double-ionized ions to 20% for which the growth rate is increased to 0.0305.

4. Rayleigh-Taylor instability

Now, for the unstable wave's potential, the perturbed part of Equation (19) is needed to be solved. From Equation (19), the perturbed part is given as

$$\frac{\partial^2 \phi_1}{\partial x^2} - k_y^2 \phi_1 + \left(\frac{k_y \xi(x) \phi_1}{\omega - k_y u_0 + \frac{\Omega^2}{\omega_{pe}^2} \left[1 - \frac{\omega_{pi}^2}{(\omega^2 - v_{thi}^2 k_y^2)} - \frac{\omega_{pzi}^2}{\omega^2} \right]} \right) \times \left(\frac{1}{\left[\omega - k_y u_0 + \frac{u_{the}^2}{\Omega^2} k_y [k_y (\omega - k_y u_0) - \xi(x)] \right]} \right) = 0 \tag{25}$$

This equation looks like the Rayleigh-Taylor instability used in fluid dynamics [8]. The above equation reduces into the Rayleigh-Taylor equation solved by Litvak and Fisch if the plasma model is considered to be cold and having only singly ionized [6].

For the density gradient driven Rayleigh-Taylor instability to exist, the phase velocity of this azimuthally propagating wave should be the same as of the electron drift velocity $\omega_R = k_y u_0$ and after one complete revolution in the azimuthal direction it should be in phase with itself i.e., $2\pi R = n\lambda$. This can also be said that as there is periodicity in the azimuthal direction [9], the azimuthal channel length, i.e., the circumference of the thruster channel, should be an integral multiple of the wavelength of the azimuthally propagating plasma unstable wave ($n\lambda = 2\pi R$), restraining wave number k_y to attain only real value while the wave frequency ω can be complex. By the Rayleigh theory from fluid dynamics [8], the necessary condition for instability to occur is to have an inflection between the boundary interval, i.e., $\xi(x_0) = 0$ should exist at some point between the anode and the virtual cathode.

As we are interested in getting an analytical solution to the

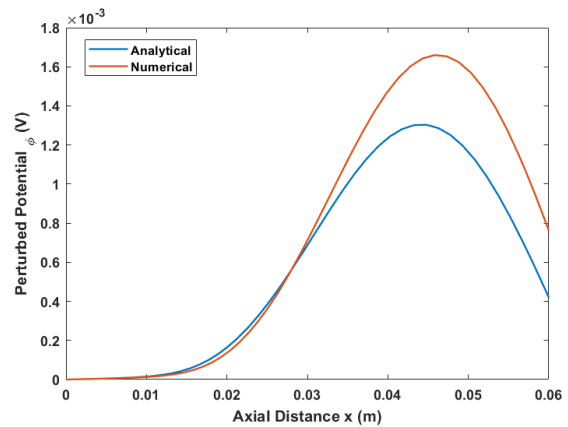


Figure 2. Comparison of analytical and numerical results.

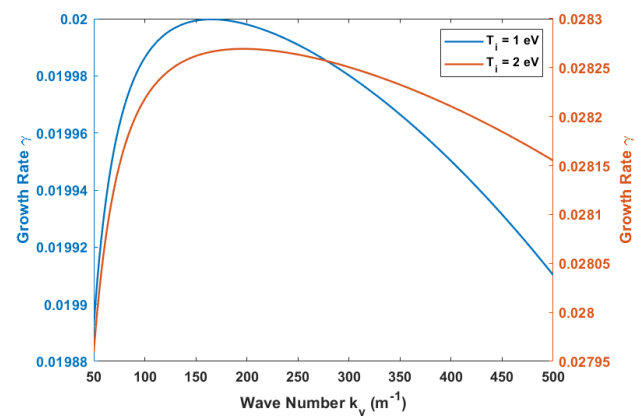


Figure 3. Weak dependence of growth rate (γ) on wave number (k_y) for two different ion temperatures (T_i).

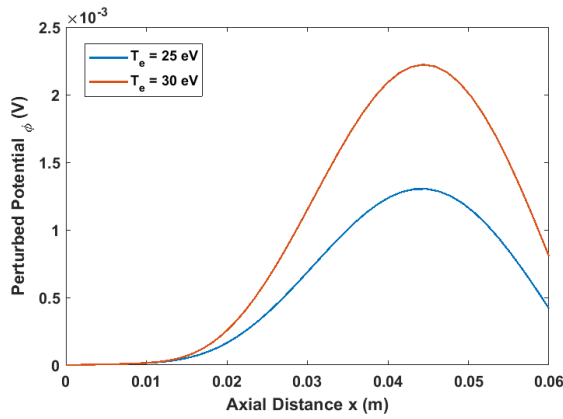


Figure 4. Perturbed potential (ϕ) profile with axial distance (x) along the channel length for two different electron temperatures (T_e).

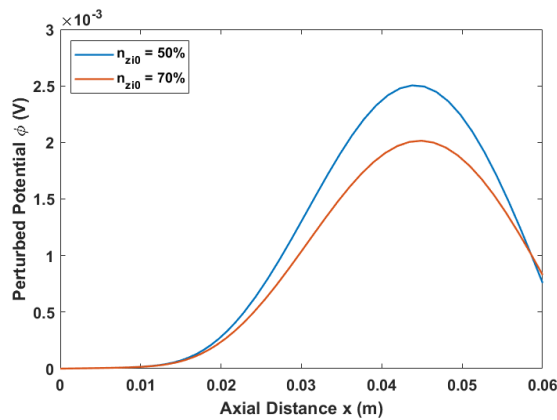


Figure 5. Perturbed potential (ϕ) profile with axial distance (x) along the channel length for two different densities of multi-ionized ions (n_{zi0}).

above equation, we rearrange it as follows

$$\frac{\partial^2 \phi_1}{\partial x^2} - k_y^2 \phi_1 + \left(\frac{k_y \frac{\xi(x)}{(\omega - k_y u_0)} \phi_1}{1 + \frac{\Omega^2}{\omega_{pe}^2} \left[1 - \frac{\omega_{pi}^2}{(\omega^2 - v_{thi}^2 k_y^2)} - \frac{\omega_{pzi}^2}{\omega^2} \right]} \times \frac{1}{\left[1 + \frac{u_{the}^2}{\Omega^2} k_y \left[k_y - \frac{\xi(x)}{(\omega - k_y u_0)} \right] \right]} \right) = 0 \tag{26}$$

Figure 4 shows the dependence of perturbed potential on the electron temperature for the same plasma parameters that are used in Figure 2, along with $k_y = 200/\text{m}$ and $T_i = 1 \text{ eV}$. The above equation can't be solved without the plasma density and electron drift velocity profiles. Based on the experimental observation, the plasma density is maximum at the position where maximum ionization of Xenon atoms takes place and electron drift velocity at the position of the maximum applied magnetic field [2]. The axial profile of the magnetic field, which confines the electrons, has a maximum in the acceleration region. These electrons are used to ionize the neutral Xenon atoms, which are injected from the anode creating plasma in the thruster's channel. So, it is appropriate to consider the plasma density and electron

drift velocity to have a Gaussian-like profile; a similar profile has been shown by Adam et al. that also supports our assumption [10]. But getting the exact profiles of density and velocity, both theoretically and numerically, are very complicated to calculate. So, for calculation purposes, we have taken a Gaussian density and drift velocity as

$$n_{e0} = n_{0 \text{ max}} \exp\left(-18\left(\frac{x-0.03}{d}\right)^2\right) \tag{27}$$

$$u_0 = u_{0 \text{ max}} \exp\left(-18\left(\frac{x-0.035}{d}\right)^2\right) \tag{28}$$

where $n_{0 \text{ max}}$ and $u_{0 \text{ max}}$ represent the maximum values of the density and the velocity, respectively, and d is the channel length. The above expressions also consider that the density distribution is such that the density reaches its maximum value slightly before the magnetic field profile or the velocity profile, since mostly neutral atoms get ionized before reaching the maximum magnetic field region. Similar distribution of the density and velocity have been shown experimentally [10].

Now we analyse the function $\xi(x)/(\omega - k_y u_0)$ (Let's say $\chi = \xi(x)/(\omega - k_y u_0)$). If one compares the function $(1/\phi_1)\partial\phi_1/\partial x (\sim 10^2)$ with the help of experimental results or numerical studies [11], to the function $(1/\chi)\partial\chi/\partial x (\sim 10^{-2})$ with the help of density and velocity profiles considered in the current problem, it is observed that χ is a slow varying function relative to the potential ϕ_1 . And if we compare both the functions, it can be shown that

$$\frac{1}{\phi_1} \frac{\partial \phi_1}{\partial x} > \frac{1}{L} > \frac{1}{\chi} \frac{\partial \chi}{\partial x} \tag{29}$$

Here L is the scale length of inhomogeneity. Thus, we can consider the slowly varying quantities as constant compared to the perturbed potential ϕ_1 . With this simplification, the solution to Equation (26) can be written in the following form

$$\phi_1 = 2C \sinh \left[\left(k_y^2 - \frac{k_y \chi}{1 + \frac{\Omega^2}{\omega_{pe}^2} \left[1 - \frac{\omega_{pi}^2}{(\omega^2 - v_{thi}^2 k_y^2)} - \frac{\omega_{pzi}^2}{\omega^2} \right]} \right)^{\frac{1}{2}} \right] \times \frac{1}{\left[1 + \frac{u_{the}^2}{\Omega^2} k_y (k_y - \chi) \right]} \tag{30}$$

using boundary conditions $\phi_1(0) = \phi_1(x_d) = 0$, where x_d is the position of the virtual cathode. Here, C is a constant of experimental fit.

5. Results

In order to verify the analytically obtained solution (30) for the perturbation potential, Equation (26) is solved numerically using initial values as $\phi_1(0) = \dot{\phi}_1(0) = 0$. The perturbed potential so obtained is plotted in Figure 2, where the potential profile obtained by the analytical approach is also plotted. There is a good agreement between the two profiles of the potential, verifying the correctness of our analytical calculations. In this figure and also at other places in the article (until specified), 60% ions are considered to

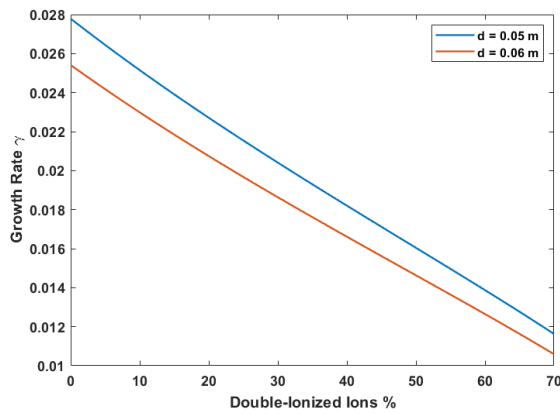


Figure 6. Dependence of growth rate (γ) on the density of double-ionized ions (n_{zI0}) for two different channel lengths (d).

be double-ionized and the plasma parameters are taken as $B_0 = 200$ G, $d = 0.06$ m, $k_y = 200/\text{m}$, $\gamma_e = \gamma_i = 2$, $T_e = 25$ eV, $T_i = 1$ eV, $M = 2.17 \times 10^{-25}$ kg, $n_{0 \max} = 10^{18}/\text{m}^3$, and $u_{0 \max} = 10^6$ m/s. These parameters have been used in Hall thruster studies and experimentally realized by Smirnov et al. and are within an acceptable range [12–14].

The necessary condition for Rayleigh-Taylor instability states that the function $\xi(x)$ must have an inflection point between the boundaries and if we observe the function $\xi(x)$ under current density and velocity profiles that are used in this article, the inflection point is found to take place at $x = 0.0298$ m. It is noticed that the function $\xi(x)$ is negative before the inflection point and is positive after this point. If we see its role in the perturbed potential profile which is calculated using it as a slowly varying function, it is seen that before the inflection point it helps increasing the magnitude of the terms inside the hyperbolic function (being negative) and after that it reduces its magnitude (being positive). This might be the cause of slight discrepancies between analytical and numerical results.

Figure 3 shows the variation of the growth rate with the wave number for two different ion temperatures for the same plasma parameters, as used in Figure 2. Here this is evident that initially, the growth rate increases with the wave number, and after achieving maximum value at a certain point, it starts decreasing. This behaviour can be explained with the help of the azimuthal drift of the electron fluid. The Rayleigh theorem from fluid dynamics states that for this azimuthal propagating wave to be unstable, the fluid velocity must be equal to the phase velocity along with the inflection point [8]. It means when $\omega_R = k_y u_0$, the growth rate reaches its maximum value. The increased growth rate with the increased ion temperature is because of the increased pressure gradient term, which acts like the increased density gradient.

The increased pressure gradient term in the electrons fluid momentum equation will act as the increased density gradient term, thus resulting in an increased perturbed potential. This result is consistent with the result obtained by Malik and Singh [15] using a numerical approach to solve the

Rayleigh-Taylor equation and experimental results obtained by Kusamoto et al. [16]. This is a point of mention that the variation of perturbed potential for the density driven or RT instability was not shown in the work of Hall thruster plasmas [17–20] and $\mathbf{E} \times \mathbf{B}$ plasmas [21, 22], contrary to the present investigation.

The axial profile of the perturbed potential and its dependence on the densities of double-ionized ions is shown in Figure 5. The plasma parameters used are the same as in Figure 2. The increased density of double-ionized ions results in a relatively smaller perturbed potential. It can be explained with the help of the reduced restoring force on the electrons due to the increased attractive force of double-ionized ions, as the double-ionized ions attract more electrons relative to the single-ionized ions. Since the ions in the Hall thruster are unmagnetized, the double-ionized ions help break the magnetic trapping of the electrons. That means it reduces the density gradient of the electrons in the channel of the thruster, resulting in a smaller perturbing potential.

Figure 6 shows the behavior of the growth rate with the density of double-ionized ions for two different thruster channel lengths. As the density of double-ionized ions increases, the growth rate decreases, and a relatively higher growth rate is observed in a thruster with a smaller channel length. The increased density of double-ionized ions reduces the density gradient, resulting in lower growth rates. With the increased channel length also, the density gradient decreases, and because Rayleigh-Taylor instability is a gradient-driven instability its growth rate decreases with the reduced density gradient, i.e. with the increase of channel length as well as the larger density of the double-ionized ions.

6. Conclusion

An azimuthally propagating wave was discussed using a three-fluid model consisting of electrons, single-ionized ions, and double-ionized ions. For this azimuthal wave, an unstable mode of frequency ω_3 was obtained, and the necessary condition ($q^2 + p^3 > 0$) for this instability was realized. The condition ($1/\phi_1(\partial\phi_1/\partial x) > 1/L > 1/\chi(\partial\chi/\partial x)$) enabled us to find the analytical solution of the modified Rayleigh-Taylor equation with the consideration of slow varying plasma parameters. Most of the results were obtained by choosing the parameters of an SPT-100 Hall thruster. The frequency of this unstable wave was found to be of the order of 10 MHz and the phase velocity (ω_R/k_y) turned out to be of the order of the electron drift velocity. Larger concentration of double-ionized ions reduced the growth rate and the perturbed potential.

Acknowledgments

The author Dhananjay Verma acknowledges the financial support provided by the University Grant Commission (UGC), Govt. of India.

Data Availability Statement

Data sharing is not applicable to this article as no datasets were generated or analysed during the current study.

Conflict of interest statement:

The authors declare that they have no conflict of interest.

References

- [1] D. M. Goebel and I. Katz. *Fundamentals of electric propulsion: ion and Hall thrusters*. John Wiley and Sons, 2008.
- [2] J. P. Boeuf. “Tutorial: Physics and modeling of Hall thrusters”. *Journal of Applied Physics*, **121**:011101, 2017.
- [3] F. Taccogna and L. Garrigues. “Latest progress in Hall thrusters plasma modelling”. *Reviews of Modern Plasma Physics*, **3**:1, 2019.
- [4] H. Kim, S. Lee, G. Doh, D. Lee, and W. Choe. “Magnetic field tailoring effects on ion beam properties in cylindrical Hall thrusters”. *Journal of Applied Physics*, **131**:033303, 2022.
- [5] A. A. Litvak, Y. Raitses, and N. J. Fisch. “Experimental studies of high-frequency azimuthal waves in Hall thrusters”. *Physics of Plasmas*, **11**:1701, 2004.
- [6] A. A. Litvak and N. J. Fisch. “Rayleigh instability in Hall thrusters”. *Physics of Plasmas*, **11**:1379, 2004.
- [7] V. H. Chaplin, L. K. Johnson, R. B. Lobbia, M. F. Konopliv, T. Simka, and R. E. Wirz. “Insights from Collisional-Radiative models of neutral and singly ionized Xenon in Hall thrusters”. *Journal of Propulsion and Power*, **38**:1, 2022.
- [8] L. D. Landau and E. M. Lifshitz. *Fluid Mechanics*. Addison Wesley, New York, 1959.
- [9] B. B. Kadomtsev. *Reviews of Plasma Physics*. Consultants Bureau, New York, 1992.
- [10] J. C. Adam, J. P. Boeuf, N. Dubuit, M. Dudeck, L. Garrigues, D. Gresillon, and S. Tsikata. “Physics, simulation and diagnostics of Hall effect thrusters”. *Plasma Physics and Controlled Fusion*, **50**:124041, 2008.
- [11] J. P. Boeuf and L. Garrigues. “ $\mathbf{E} \times \mathbf{B}$ electron drift instability in Hall thrusters: Particle-in-cell simulations vs. theory”. *Physics of Plasmas*, **25**:1, 2018.
- [12] A. Smirnov, Y. Raitses, and N. J. Fisch. “Parametric investigation of miniaturized cylindrical and annular Hall thrusters”. *Journal of Applied Physics*, **92**:5673, 2002.
- [13] E. Chesta, N. B. Meezan, and M. A. Cappelli. “Stability of a magnetized Hall plasma discharge”. *Journal of Applied Physics*, **89**:3099, 2001.
- [14] G. J. M. Hagelaar, J. Bareilles, L. Garrigues, and J. P. Boeuf. “Role of anomalous electron transport in a stationary plasma thruster simulation”. *Journal of Applied Physics*, **93**:67, 2003.
- [15] H. K. Malik and S. Singh. “Conditions and growth rate of Rayleigh instability in a Hall thruster under the effect of ion temperature”. *Physical Review E*, **83**:036406, 2011.
- [16] D. Kusamoto, K. Mikami, K. Komurasaki, and A. D. Gallimore. “Exhaust beam profiles of Hall thrusters”. *Trans. of Japanese Soc. for Aeronautical and Space Sci.*, **40**:238, 1998.
- [17] H. K. Malik, J. Tyagi, and D. Sharma. “Growth of Rayleigh instability in a Hall thruster channel having dust in exit region”. *AIP Advances*, **9**:1, 2019.
- [18] J. Tyagi, D. Sharma, and H. K. Malik. “Discussion on Rayleigh equation obtained for a Hall thruster plasma with dust”. *Journal of Theoretical and Applied Physics*, **12**:227, 2018.
- [19] S. Singh and H. K. Malik. “Role of ionization and electron drift velocity profile to Rayleigh instability in a Hall thruster plasma”. *Journal of Applied Physics*, **112**:1, 2012.
- [20] S. P. Bharti and S. Singh. “The spatial damping of electrostatic wave in Hall thruster beam plasma”. *Journal of Theoretical and Applied Physics*, **16**:1, 2022.
- [21] Munish, R. Dhawan, R. Kumar, and H. K. Malik. “Density gradient driven instability in an $\mathbf{E} \times \mathbf{B}$ plasma system having temperature gradients”. *Journal of Taibah University for Science*, **16**:725, 2022.
- [22] R. Dhawan, D. Sharma, and H. K. Malik. “Influence of magnetic field and ionization on gradient driven instability in an $\mathbf{E} \times \mathbf{B}$ plasma”. *Journal of Theoretical and Applied Physics*, **16**:1, 2022.